Supplement of Atmos. Chem. Phys., 18, 1065–1078, 2018
https://doi.org/10.5194/acp-18-1065-2018-supplement

Atmospheric Chemistry and Physics
Open Access
EGU

Supplement of

Impact of aerosols on ice crystal size

B. Zhao et al.

Correspondence to: Bin Zhao (zhaob1206@ucla.edu) and Yu Gu (gu@atmos.ucla.edu)

Figures and Tables

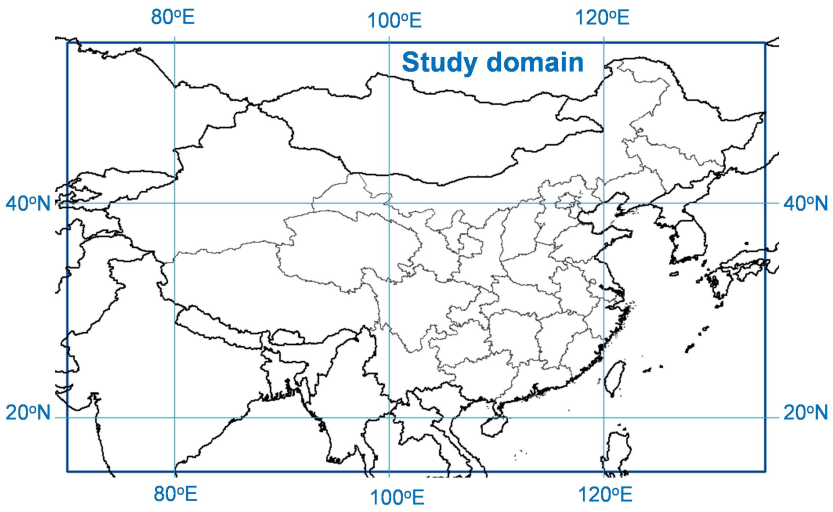

Figure S1. The spatial domain of this study: 15º-55º N, 70º-135º E.

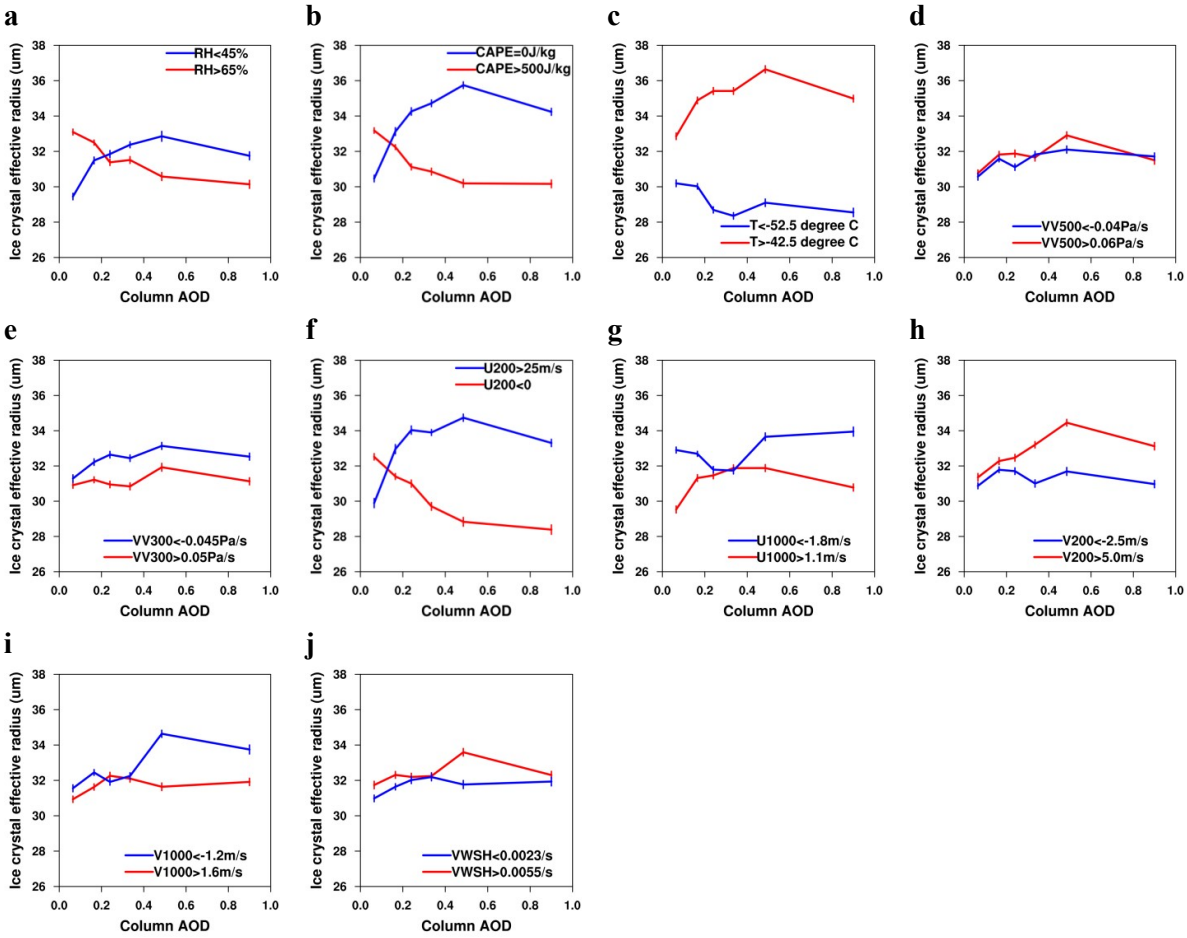

Figure S2. Changes in R_{ei} as a function of AOD for different ranges of (a) relative humidity averaged between 100 hPa and 440 hPa ($RH_{100\text{-}440hPa}$), (b) the convective available potential energy (CAPE), (c) the middle cloud layer temperature (T_{mid}), (d) the pressure vertical velocity at 500 hPa (VV500), (e) the pressure vertical velocity at 300 hPa (VV300), (f) the U-components of wind speed at 200 hPa (U200), (g) the U-components of wind speed at 1000 hPa (U1000), (h) the V-components of wind speed at 200 hPa (V200), (i) the V-components of wind speed at 1000 hPa (V1000), (j) and the vertical wind shear (VWSH) at potential vorticity surface of 2×10^{-6} deg K m^2 kg^{-1} s^{-1}. The meteorological parameters are divided into 3 ranges containing similar numbers of data points, and the curves for the medium meteorological range are not shown. The definition of error bars is the same as in Fig. 1 in the main text. The total number of samples used in this figure is 5.68×10^4.

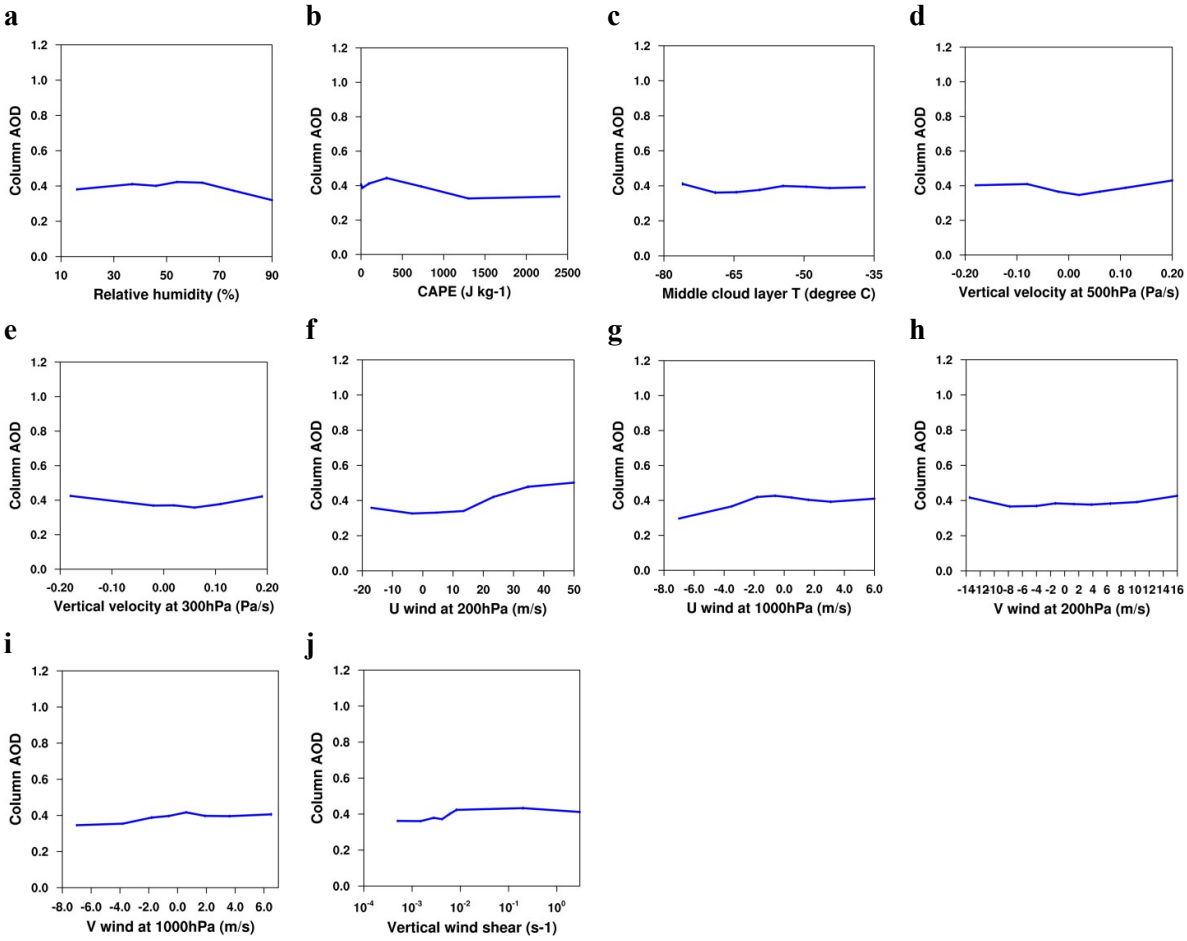

Figure S3. Changes in AOD as a function of meteorological parameters: (a) $RH_{100\text{-}440hPa}$, (b) CAPE, (c) T_{mid}, (d) VV500, (e) VV300, (f) U200, (g) U1000, (h) V200, (i) V1000, and (j) VWSH at the potential vorticity surface of 2×10^{-6} deg K m^2 kg^{-1} s^{-1}. The definition of error bars is the same as in Fig. 1 in the main text. Note that the error bars in some panels are very small and hence not visible. The total number of samples used in this figure is 5.68×10^4.

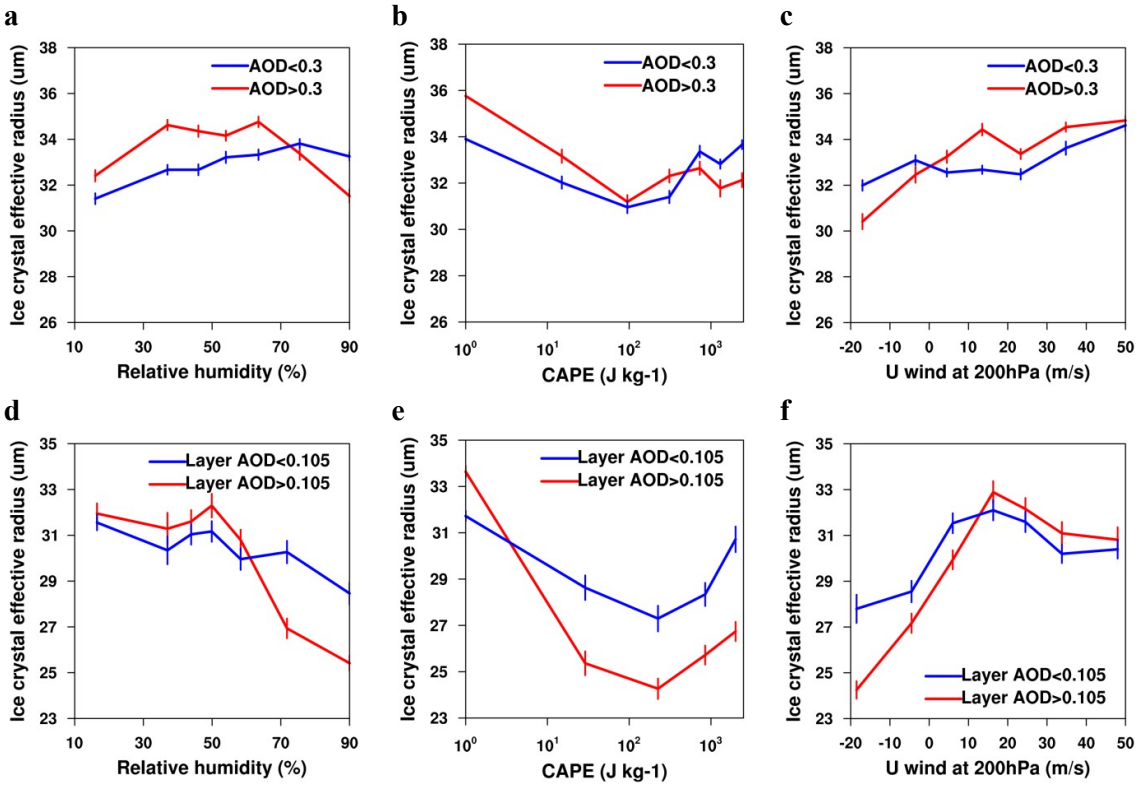

Figure S4. Changes in R_{ei} with meteorological parameters for different ranges of aerosol loading. (a-c) Changes in R_{ei} of convection-generated ice clouds with (a) $RH_{100\text{-}440hPa}$, (b) CAPE, and (c) U200 for different ranges of AOD. (d-f) Changes in R_{ei} of in-situ ice clouds with (d) $RH_{100\text{-}440hPa}$, (e) CAPE, and (f) U200 for different ranges of layer AOD. All samples are divided into two AOD ranges containing similar sample numbers. The definition of error bars is the same as in Fig. 1. The total numbers of samples used for convection-generated and in-situ ice clouds are 2.73×10^4 and 1.09×10^4, respectively.

Table S1. Datasets used in this study.

Satellite/ Sensor	Product	Variable	Horizontal resolution
Aqua/MODIS	MYD04 (Level 2, Collection 6)	Column AOD	10 km × 10 km
	MYD06 (Level 2, Collection 6)	Cloud effective radius, cloud phase (determined by the "cloud optical property" algorithm), primary cloud retrieval outcome, Cloud effective radius uncertainty	1 km × 1 km
CALIPSO/ CALIOP	05kmMLay (Level 2, Version 4.10)	Aerosol/cloud layer number, layer base temperature, middle layer temperature, layer top/base height, layer aerosol/cloud optical depth, feature classification flags, CAD score, extinction QC	5 km along-track
	05kmAPro (Level 2, Version 4.10)	Vertically resolved pressure, relative humidity, and temperature	5 km along-track
--	NCEP ds083.2	Vertically resolved pressure vertical velocity and wind speed; CAPE, wind shear	1º × 1º

Table S2. Correlation coefficients between various meteorological parameters.

	$RH_{100\text{-}440hPa}$	CAPE	U200	T_{mid}
$RH_{100\text{-}440hPa}$	--	0.514	-0.535	-0.352
CAPE	0.514	--	-0.623	-0.390
U200	-0.535	-0.623	--	0.502
T_{mid}	-0.352	-0.390	0.502	--

Note: $p < 0.01$ for all cases. $RH_{100\text{-}440hPa}$, relative humidity averaged between 100 hPa and 440 hPa; CAPE, convective available potential energy; U200, U-components of wind speed at 200 hPa; T_{mid}, middle cloud layer temperature.